

# New measurements of the water vapor continuum in the region from 0.3 to 2.7 THz

V.B. Podobedov<sup>a,\*</sup>, D.F. Plusquellic<sup>a</sup>, K.E. Siegrist<sup>a</sup>,  
G.T. Fraser<sup>a</sup>, Q. Ma<sup>b</sup>, R.H. Tipping<sup>c</sup>

<sup>a</sup>*Optical Technology Division, National Institute of Standards and Technology, Gaithersburg, MD 20899, USA*

<sup>b</sup>*NASA Goddard Institute for Space Studies, and Department of Applied Physics and Applied Mathematics, Columbia University, 2880 Broadway, New York, NY 10025, USA*

<sup>c</sup>*Department of Physics and Astronomy, University of Alabama, Tuscaloosa, AL 35487, USA*

Received 5 February 2007; received in revised form 9 July 2007; accepted 11 July 2007

## Abstract

We present a spectroscopic study of the water vapor continuum absorption in the far-IR region from 10 to 90 cm<sup>-1</sup> (0.3–2.7 THz). The experimental technique combines a temperature-stabilized multipass absorption cell, a polarizing (Martin–Puplett) interferometric spectrometer, and a liquid-He-cooled bolometer detector. The contributions to the absorbance resulting from the structureless H<sub>2</sub>O–H<sub>2</sub>O and H<sub>2</sub>O–N<sub>2</sub> continua have been measured in the temperature range from 293 to 333 K with spectral resolution of 0.04–0.12 cm<sup>-1</sup>. The resonant water vapor spectrum was modeled using the HITRAN04 database and a Van Vleck–Weisskopf lineshape function with a 100 cm<sup>-1</sup> far-wing cut-off. Within experimental uncertainty, both the H<sub>2</sub>O–H<sub>2</sub>O and H<sub>2</sub>O–N<sub>2</sub> continua demonstrate nearly quadratic dependencies of absorbance on frequency with, however, some deviation near the 2.5 THz window. The absorption coefficients of 3.83 and 0.185 (dB/km)/(kPa THz)<sup>2</sup> were measured for self- and foreign-gas continuum, respectively. The corresponding temperature exponents were found to be 8.8 and 5.7. The theoretically predicted foreign continuum is presented and a reasonable agreement with experiment is obtained.

© 2007 Elsevier Ltd. All rights reserved.

*Keywords:* Continuum; IR; THz; Nitrogen; Water vapor; Atmosphere

## 1. Introduction

The significant dependence of the atmospheric absorption on humidity is an important factor affecting the accuracy of ground-based radio astronomy and satellite-based spectroscopic applications [1]. In many regions, the water vapor absorption spectrum strongly contributes to the baseline absorption used as a background signal. In the far-IR region, due to the large number of strong rotational lines of water vapor, most of the observations will be mainly limited to a few relatively transparent windows shown in Fig. 1. To lower the impact of humidity over an absorbing pathlength, a few ground-based facilities including ALMA in northern

\*Corresponding author. Tel.: +1 301 975 4253; fax: +1 301 869 5700.

E-mail address: [Vyacheslav.Podobedov@nist.gov](mailto:Vyacheslav.Podobedov@nist.gov) (V.B. Podobedov).

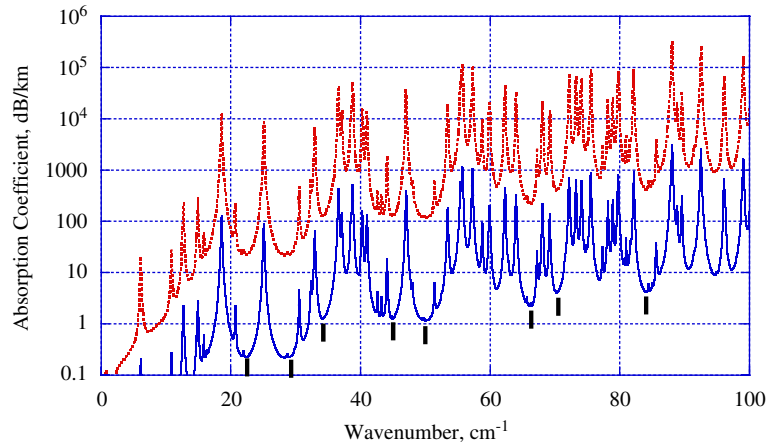


Fig. 1. Expected absorption coefficient at 0.25% (lower spectrum) and 25% relative atmospheric humidity at  $T = 296$  K. Continuum absorption is not included. The vertical bars indicate the windows considered in this paper.

Chile and Mauna Kea Observatory were developed in unusually high and dry locations. Nevertheless, reliable calibration data for atmospheric transmittance in THz window regions are required for a wide range of temperatures and relative humidities [2].

From the experimental point of view, the continuum absorbance is defined as the difference between the measured absorbance and contributions to the absorbance from local lines, calculated based on a specified resonance spectrum model. The latter is usually characterized by a database (consisting of frequencies, intensities, and shape parameters for individual lines), an upper frequency cut-off to limit the local lines included in the model, and a line-shape function (such as the VVW shape commonly adopted). Sometimes, an additional cut-off is introduced on the line far-wing shapes beyond which their magnitudes are set to be zero. It should be mentioned that any reasonable choice of the model parameters are applicable. However, a crucial point regarding any discussion of continuum absorbance is the complete specification of the resonance spectrum model used. Given the fact that in the THz windows, local line contributions dominate the absorbance and different resonance spectrum models could yield quite different local line contributions; therefore, the continuum values derived from the same raw data depend sensitively on the resonance spectrum model selected. Variation of continuum data due to the choice of the spectroscopic database and line-shape parameters was previously demonstrated in Refs. [3–6].

In the present study, we prefer to choose the two cut-offs mentioned above based on experimental accuracy considerations. This means that both cut-offs may be reasonably limited whereupon further increases make only minor contributions compared to the measurement uncertainty. In particular, it was found in Ref. [3] that the increase of the far-wing cut-off beyond  $100\text{ cm}^{-1}$  had no practical effect. Meanwhile, we would like to use the most updated database in calculating resonance spectrum.

Most continuum studies, both theoretical and experimental, have been performed in the microwave region below  $350\text{ GHz}$  [5–7], while only a few data are available above this frequency [4,8–10], and no experimental data are reported between  $55$  and  $100\text{ cm}^{-1}$ . For a typical continuum absorption coefficient, e.g.,  $k_c(\nu, T) < 10^{-5}\text{ cm}^{-1}$ , the measurement of such a weak absorption is possible mostly with long optical pathlengths that can be realized in situ, as well as in laboratory multipass cells [3] or microwave cavity devices [6]. Certainly, laboratory conditions provide better control of the basic parameters of the absorbing media such as pressure and temperature. Recently, we have reported the broadband measurements of the water vapor continuum in the  $12\text{--}55\text{ cm}^{-1}$  spectral region [3]. Those measurements were performed at a fixed temperature of  $T = 297\text{ K}$ . An extension of both the frequency and temperature ranges of the continuum measurements is needed for validation of different models.

This paper addresses the needs of both terrestrial and satellite programs for an accurate model of the water vapor continuum in a far-IR region up to  $2.7\text{ THz}$ . To achieve these goals, we utilize an experimental

spectroscopic method, employing a broadband Fourier transform spectrometer and a temperature-controlled multipass cell to enhance absorption. Resonance water vapor spectra were modeled with the latest HITRAN04 database updated for the self-broadening parameters in the THz region. The absorbance due to both H<sub>2</sub>O–H<sub>2</sub>O and H<sub>2</sub>O–N<sub>2</sub> continua was measured in the temperature range from 293 to 333 K. The experimental continuum absorption coefficients and the exponent  $n$  representing the  $(300/T)^n$  dependence of the continuum absorbance on temperature were obtained from fits in individual windows and from global fits that covered all windows with an assumed  $\nu^2$  frequency-dependent formula.

## 2. Experiment

The detailed description of multipass cells used in these experiments was presented in Ref. [3]. The basic design has a typical white cell configuration [11,12] with a 60-mm input aperture and  $f/2$  optics to compensate for the expected diffraction losses in the low-frequency end of the operational range. Gold-coated mirrors were used throughout to minimize the reflection losses in the far-IR. The upper limit for the operational range of the polarizing (Martin–Puplett) interferometric spectrometer was set to  $125\text{ cm}^{-1}$  and the high-frequency radiation was attenuated by a long-pass filter to avoid additional background noise in the range below  $90\text{ cm}^{-1}$  where the measurements were performed. The actual filter cut-off was chosen as a compromise between filter efficiency in the operational range and attenuation of blocked radiation. The coupling optics were designed to provide minimum losses of signal between the cell and spectrometer. The effective cell pathlength for this experiment is 23.3(2) m. This value differs from 24 m for 40 passes defined by geometrical optics [3].

For these measurements, the major upgrade to the multipass cell is a stabilized temperature control unit. Twelve silicon rubber heaters, two on each side of an aluminum 70-l box, serve to provide maximum uniform heating. To avoid any expansion stress and temperature gradients, the heating rate was maintained at about  $5^\circ\text{C}/\text{h}$ . This accounts for the heat supplied to the multipass cell itself (internal part of design) and environmental contact losses. Two thermometers attached to the box and to the cell optics provided independent temperature measurements. Normally, during the measurements, the difference between the readings of two thermometers did not exceed  $0.4^\circ\text{C}$  after sample equilibration. The operational temperature was considered as the average value of two readings. Because the whole system is surrounded by a thermoinsulation cover to improve uniformity of heating, the uncertainty in a measured temperature is expected to be about  $0.2^\circ\text{C}$ . The maximum operational temperature is limited primarily by the material used for both the input and output windows. In the range from 10 to  $90\text{ cm}^{-1}$ , the best material was found to be a high-density polyethylene. While its melting point is about  $135^\circ\text{C}$ , polyethylene softens at much lower temperatures and may distort when the chambers are at different pressures. For this reason, temperatures above  $70^\circ\text{C}$  were not applied.

A typical measurement session consisted of the following steps. The cell was filled with gaseous He for better heat transfer and stabilized at the operational temperature for a few hours. Then a total of four consecutive spectra were recorded including (i) a reference spectrum with the cell evacuated below 0.1 Pa, (ii) the sample spectra of H<sub>2</sub>O vapor, (iii) H<sub>2</sub>O–N<sub>2</sub> mixture, and finally (iv) a second reference spectrum. Sample mixtures were prepared by evaporation of triply distilled water mixed with high-purity nitrogen (99.9999% purity). Normally, the temperature stabilization of the gas mixture takes about 0.5–1 h, thus increasing a session time beyond that required for recording the spectrum. It is therefore important to have two reference spectra that characterize the dynamics of the instrumental drift in order to get a better measure of the minimum uncertainty of the measured absorbance. Based on a compromise between baseline drift, signal-to-noise ratio and required resolution, most spectra were obtained with a spectral resolution of  $0.12\text{ cm}^{-1}$ . The baseline drift is the largest instability component and caused an error of about  $\pm 0.006$  on the scale of measured absorbance from 0 to 1. Originating from the instrument and related software used here, the absorbance,  $A$ , is expressed as  $A = \log_{10}(1/T)$ , where the maximum transmittance,  $T$ , is equal to unity. For convenience, the second scale in dB/km is also presented. For the pathlength used here (23.3 m), the absorbance of  $A = 1$  corresponds to absorption coefficient of 429 dB/km.

### 3. Results and discussion

Continuum absorption was measured in a few windows centered at 22.5, 28.3, 34.3, 45.0, 50.3, 66.4, 70.1 and 84.1  $\text{cm}^{-1}$ . These regions are located near the minimum absorbance between strong resonance water lines (see Fig. 1). A detailed description of the retrieval of the continuum absorbance from the raw data can be found elsewhere [3]. In this study, all the individual line parameters for water vapor in the THz range were taken directly from HITRAN04 database. The resonance absorption spectra of water vapor were modeled by the JB95 program [13] using a 100  $\text{cm}^{-1}$  far-wing cut-off for a Van Vleck–Weisskopf lineshape [14] and a 185  $\text{cm}^{-1}$  high-frequency cut-off. The intensity was set to zero beyond the far wing cut-off and no resonance water vapor lines were taken into account beyond the high-frequency cut-off. The program input parameters included pressure, temperature, pathlength, lineshape, far-wing cut-off and high-frequency cut-off factors.

The total absorbance  $A$  of an  $\text{H}_2\text{O}$ – $\text{N}_2$  mixture has two parts, which are measured in the experiment as their sum,

$$A(\nu, T) = A_L + A_C, \quad (1)$$

where the indexes L and C specify a local contribution from the discrete water vapor spectrum and continuum absorption, respectively. The continuum part,  $A_C$ , may be described by the combination of three components

$$A_C(\nu, T) = A_{\text{self}}(P_{\text{H}_2\text{O}}^2) + A_{\text{foreign}}(P_{\text{N}_2} P_{\text{H}_2\text{O}}) + A_{\text{foreign}}(P_{\text{N}_2}^2), \quad (2)$$

some of which, depending on the composition of the mixture, may be neglected due to their small relative value. In our case, where the water vapor content is high (wet continuum), the third term in Eq. (2) will be significantly smaller than the remaining two. Indeed, within the experimental uncertainty, no absorption in pure nitrogen was detected. Furthermore, due to the different pressure dependence of the self- and foreign-continua, the latter becomes dominant at the low water content of the mixture. A more detailed formula describing the absorption of the  $\text{H}_2\text{O}$ – $\text{N}_2$  mixture accounts for the absorption coefficients and temperature exponents for water vapor and foreign gas separately [5,6]:

$$A_C(\nu, T) = [K_{\text{self}}(\nu)(300/T)^{n_s} + K_{\text{for}}(\nu)(300/T)^{n_f}] \nu^2 L, \quad (3)$$

where  $K_{\text{self}}(\nu)$  and  $K_{\text{for}}(\nu)$  are the absorption coefficients, respectively,  $\nu$  is the frequency and  $L$  is the pathlength.

#### 3.1. Self-continuum

The summary of self-continuum data is presented in Fig. 2 and Table 1. As seen from these data, with an exception of the window at 84.1  $\text{cm}^{-1}$ , most of the data may be satisfactorily fitted by a simple function reflecting a nearly quadratic dependence of self-continuum absorbance on frequency. Such a trend is observed in the microwave [5,15], but deviations from this quadratic dependence in the submillimeter and the far-IR regions were also reported [16,17]. In particular, the model used in Ref. [16] predicts a lower rise of the continuum in the region close to its maximum value at about 120  $\text{cm}^{-1}$ . As seen from Fig. 2, with an extension of the range toward higher frequencies, up to 90  $\text{cm}^{-1}$  in our case, the deviation from  $\nu^2$ -function appears to increase and exceeds the experimental uncertainty. At this point, there are two choices for the treatment of the experimental data. The first one comprises consideration of individual windows separately. In this case, the data in each window are fitted with a  $A(300/T)^n$  function, where  $A$  and  $n$  would be absorbance and temperature exponent, respectively. In the second case, the absorbance data for single temperature are first fitted to a  $\nu^2$ -function. Then the fit over temperature is performed as described above. Notice that in this latter case, the absorbance,  $A$ , is taken from more data already fitted with a  $\nu^2$ -function.

For this analysis, we therefore perform both the individual fits to the data in each window and a quadratic fit in the range up to 70.1  $\text{cm}^{-1}$ . By carrying out fits for each of the windows, the self-continuum absorption coefficients and the temperature dependence index  $n_s$  can be derived and are presented in Table 1. Meanwhile, by assuming a  $\nu^2$ -dependence of the absorption, the self-continuum absorption coefficient found may be presented as  $K_{\text{self}} = 3.83 \text{ (dB/km)/(kPa THz)}^2$  within the range from 10 to 70.1  $\text{cm}^{-1}$ . A small deviation from the value reported in Ref. [3] is likely due to differences between the explicit self-broadening parameters used

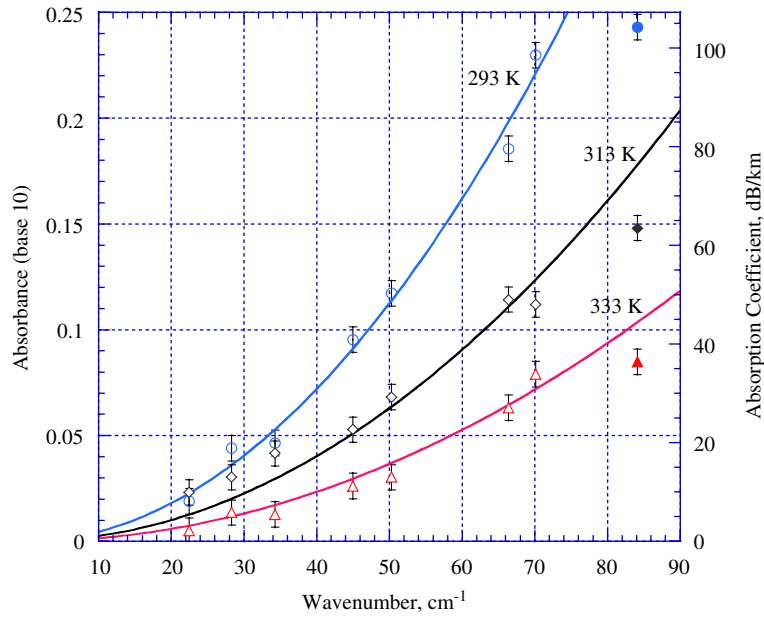


Fig. 2. Self-continuum absorption of water vapor at  $P = 2.13$  kPa at different temperatures. Data for the  $84.1 \text{ cm}^{-1}$  window are not included in the  $\nu^2$ -fit presented by solid curves.

Table 1

Experimental self-continuum absorption coefficient,  $K_{\text{self}}$  (dB/km)/(kPa THz)<sup>2</sup> and temperature exponent,  $n_s$ , obtained from each transmittance window. The same parameters shown below the dashed line were determined from the complete set of  $\nu^2$ -fitted curves (see Fig. 2)

Window center ( $\text{cm}^{-1}$ )	$K_{\text{self}}$	$n_s$
22.5	3.94	5.4
28.3	4.91	7.8
34.3	3.75	6.8
45.0	3.94	9.6
50.3	3.89	9.5
66.4	3.66	8.0
70.1	3.89	9.3
84.1	2.98	7.9
-----		
$\nu^2$ -fitted	$3.83(300/T)^{8.8}$	8.8

Note: The theoretically predicted values of  $K_{\text{self}}$  and  $n_{\text{self}}$  are missing in Table 1 because the  $\text{H}_2\text{O}$ – $\text{H}_2\text{O}$  system is more complicated than the  $\text{H}_2\text{O}$ – $\text{N}_2$ , and theoretical calculations have not been completed yet.

in HITRAN04 database and the scaling parameter of 4.8 ( $\times$  air-broadening parameter) used in HITRAN01 to describe self-broadening. It should be noticed that the minimum uncertainty in the whole range from 10 to  $90 \text{ cm}^{-1}$  was reached at a relatively high pressure of water vapor of 2.13 kPa. This is due to the use of the optimum range of the measured absorbance near the maximum values of 1–1.2. At the same time, the lowest measured absorbance should reasonably exceed the experimental uncertainty caused mainly by baseline drift.

### 3.2. Foreign continuum

Typical far-IR absorption spectra of  $\text{H}_2\text{O}$ – $\text{N}_2$  mixture are presented in Fig. 3. As the temperature increases, the absorbance in all windows becomes lower indicating reduced contributions from both the local and

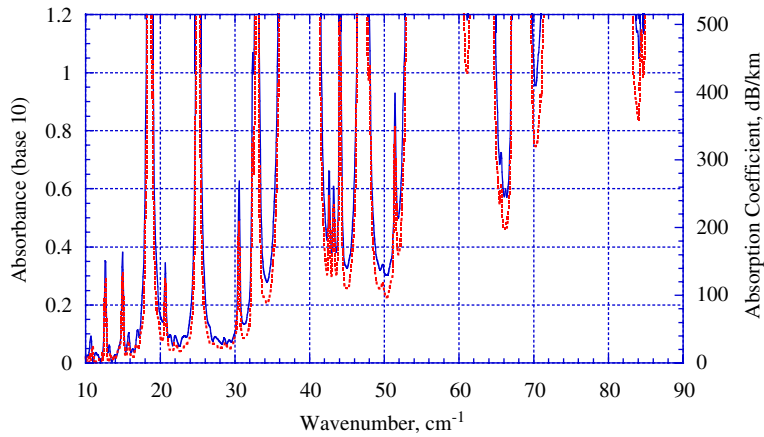


Fig. 3. Absorption spectra of a mixture composed of water vapor at 0.67 kPa and nitrogen at 70 kPa. Top and bottom spectra were obtained at 293 and 333 K, respectively.

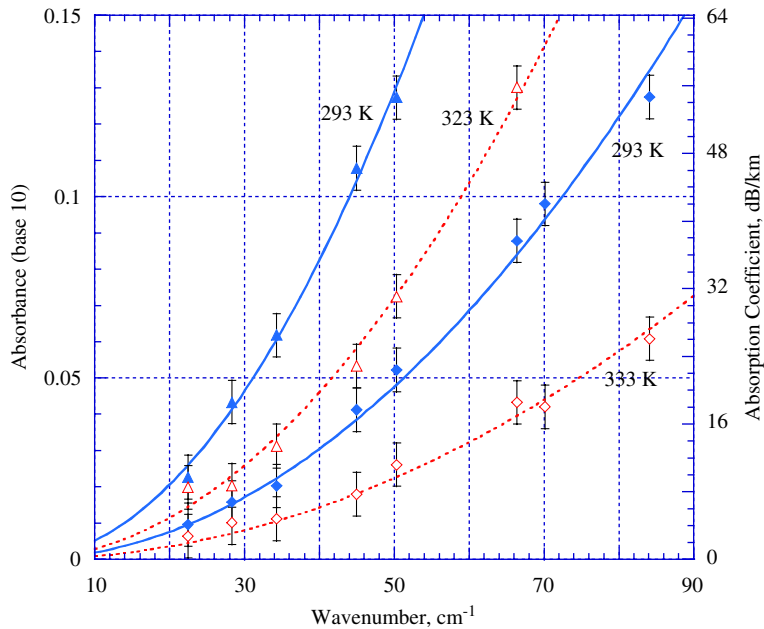


Fig. 4. Foreign continuum data for two different mixtures of H<sub>2</sub>O/N<sub>2</sub>: 1.43/78.5 kPa (triangles) and 0.67/70 kPa (rhombs). For clarity, only the end-temperature data are shown. The curves present the  $\nu^2$ -fit of absorbance data over all available windows.

continuum absorption. For the mixture composed of 0.67 kPa of water vapor and 70 kPa of nitrogen, the simultaneous measurements of absorbance are available in all windows. Further increases in pressure benefits the low-frequency measurements but leads to saturation effects at the high-frequency end of the spectrum. We use the following two sets of data obtained for different H<sub>2</sub>O/N<sub>2</sub> mixtures: 0.67 kPa/70 kPa and 1.43 kPa/78.5 kPa, together with the previously measured self-continuum absorbance for each water vapor pressure.

Fig. 4 presents the data on the foreign continuum absorption as a function of mixture composition and temperature. For clarity, only the end-temperature data and a few fitting curves are shown. Compared to the self-continuum absorbance shown in Fig. 2, a smaller deviation of the data from the  $\nu^2$ -dependence in the 84.1 cm<sup>-1</sup> window was observed. We believe this may be due to the remaining uncertainties in the

self-broadening parameters in the far-IR. The absorption coefficients for the foreign continuum were found from the fitted parameters and averaged over two sets of data assuming that the continuum scales as a product of pressures,  $P_{\text{H}_2\text{O}} \times P_{\text{N}_2}$ . From the present study, the value over all windows was best defined by  $K_{\text{for}} = 0.185(300/T)^{5.7}$  (dB/km)/(kPa THz)<sup>2</sup>. This value is presented in Table 2 along with the set of absorption coefficients found from individual windows as described in Section 3.1.

The value of the continuum temperature exponent of 5.7 was also derived from absorbance data in all available windows preliminary fitted with a  $v^2$  function. The related temperature dependence is shown by the solid curve in Fig. 5. The other dashed curves illustrate the  $(300/T)^n$  fit of the continuum absorbance in single windows over the different temperatures. Each curve is normalized so that unity of the absorbance factor occurs at 300 K. The temperature exponents found from the single windows range from 4.1 (at 22.5 cm<sup>-1</sup>) to 6.3 (at 45.0 cm<sup>-1</sup>) as shown in Table 2. This difference may be due to both the experimental uncertainty and to the individual nature of the continuum in these windows.

Table 2

Foreign continuum absorption coefficient,  $K_{\text{for}}$  (dB/km)/(kPa THz)<sup>2</sup> and temperature exponent,  $n_f$ , obtained from each transmittance window. The same parameters shown below the dashed line were determined from the complete set of  $v^2$ -fitted curves (see Fig. 4)

Window center (cm <sup>-1</sup> )	$K_{\text{for}}$		$n_f$	
	Exp.	Theory	Exp.	Theory
22.5	0.178	0.178	4.1	5.02
28.3	0.178	0.188	4.3	4.75
34.3	0.169	0.175	4.6	4.83
45.0	0.188	0.177	6.3	4.28
50.3	0.186	0.177	5.8	4.29
66.4	0.182	0.163	5.7	3.94
70.1	0.183	0.176	6.2	4.03
84.1	0.172	0.172	5.4	4.07
-----				
$v^2$ -fitted (Exp.)	0.185(300/T) <sup>5.7</sup>		5.7	

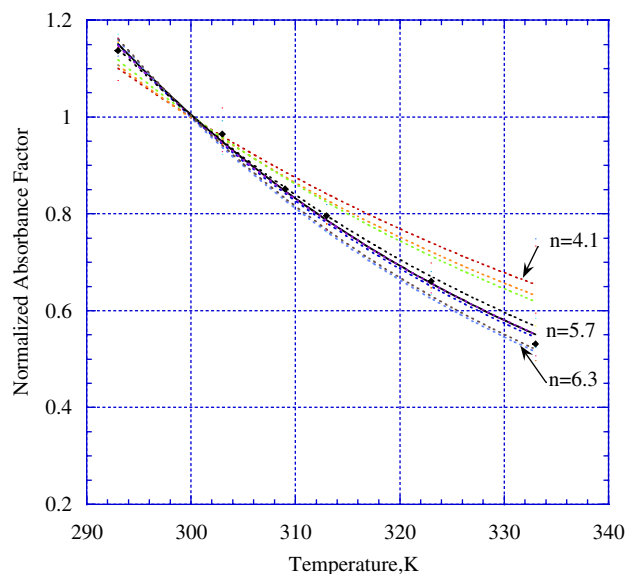


Fig. 5. Fit of the foreign continuum data to a  $(300/T)^n$  function. The solid curve is based on the data smoothed by the  $v^2$ -fit over all windows. Dashed curves demonstrate the scatter of the exponent  $n$  when obtained from a single window.

#### 4. Theoretical method in calculating the foreign continuum

A few years ago, two of the present authors have developed a theoretical method based on the Lanczos algorithm to calculate the continuum for the H<sub>2</sub>O–N<sub>2</sub> pair in the microwave region [7]. The method is based on the idea that because the microwave windows are on the low-frequency side of the pure rotational band of H<sub>2</sub>O, one can treat the band as a whole and calculate the pressure-broadened absorptions directly without accounting for contributions from each of the individual lines. As a result, the sharp absorption features of the individual lines have been averaged out, and the theoretically calculated values of the continuum vary smoothly with the frequency and can be compared with measured results. As shown in Ref. [18], the derived theoretical values in the windows below 1000 GHz agree with Liebe's semi-empirical MPM results and the experimental measurements of Bauer and co-workers reasonably well. However, this method is not applicable for THz windows because the latter are located within the pure rotational band. Fortunately, for the THz windows of interest in the present study (i.e., below 2.7 THz), most of strong lines of H<sub>2</sub>O are still located on the high-frequency side. As a result, one is able to make modifications in the Lanczos method and extend theoretical calculations into these THz windows. In practice, one divides the pure rotational band into two parts: a major part that consists of lines whose frequencies are higher than a given window, and a minor part consisting of the lower-frequency lines. Then, one can apply the Lanczos method to the major part and treat the minor part as individual local lines. A more detailed discussion of the extension of the Lanczos method is presented elsewhere later.

As mentioned previously, the continuum and the local contributions in a given window are intertwined. Therefore, it is necessary also to specify how the local contributions are calculated when we present theoretical results, and thus a new problem arises. From the theoretical point of view, different windows should have different upper-frequency cut-offs (i.e., the frequency range above the window frequency beyond which the local contributions are excluded). Unfortunately, with the present Lanczos method one can only estimate ranges of the upper-frequency cut-off,  $v_{\text{cut}}$ , for each of the windows, but not to determine this value exactly. As a result, these upper-frequency cut-offs become adjustable parameters. It is worth mentioning that the upper-frequency cut-offs discussed here differ from those introduced previously when one derives measured continuum results. But, once the former have been selected, there is no problem to adjust the theoretical continuum values to match the same cut-off used to find the measured continuum. This can be easily done by subtracting an amount of absorptions representing the differences between the spectrum used to analyze the raw data and the theoretically predicted spectrum from the original theoretical continuum values. More specifically, the formula used to account for the differences between two local line absorptions is given by

$$n \frac{1}{\pi} \sum_k S_k \frac{v}{v_k} \left[ \frac{\Delta v_k}{(v - v_k)^2 + \Delta v_k^2} + \frac{\Delta v_k}{(v + v_k)^2 + \Delta v_k^2} \right] \quad \text{with } v_{\text{cut}} < v_k \leq 185 \text{ cm}^{-1}, \quad (4)$$

where  $n$  is the number density of H<sub>2</sub>O,  $S_k$  are the line intensities, and  $\Delta v_k$  are the line widths. It is obvious that as the  $v_{\text{cut}}$  varies, this amount varies too. For the present theoretical values listed in Table 2, the  $v_{\text{cut}}$  has been treated as adjustable parameters to optimize the theoretical results to get the best agreement with the measured continuum values. Therefore, we note that due to this optimization procedure, the current theoretical continuum thus contains an empirical feature.

#### 5. Conclusions

The THz techniques presented here have permitted broadband measurements of absorption coefficients for both the H<sub>2</sub>O–H<sub>2</sub>O and H<sub>2</sub>O–N<sub>2</sub> continua under well-controlled laboratory conditions. The temperature dependence of both the self- and foreign-continuum of water vapor have been studied in a multipass cell using broadband spectroscopic data and the HITRAN04 database. The data are available in the range from 10 to 90 cm<sup>-1</sup> (0.3–2.7 THz) and temperatures from 293 to 333 K. Both self- and foreign-continua exhibit a nearly quadratic dependence of absorption on the frequency with an exception of the highest window at 84.1 cm<sup>-1</sup>. The absorption coefficients and temperature exponents were found from the complete set of experimental absorbance data and from the fit of continuum absorbance in a single window over different temperatures.

Table 3

Comparison of the continuum absorption coefficients,  $K_{\text{self}}$  and  $K_{\text{for}}$ , (dB/km)/(kPa THz)<sup>2</sup> and temperature exponents,  $n_s$  and  $n_f$  from different studies

Reference range, THz	[5] <0.8	[6] <0.35*	[4] 0.35–1.1	[16]**	Present work 0.3–2.7		
					Experiment		Theory
					(a)	(b)	(c)
$K_{\text{self}}$	7.8	8.9–9.5	–	4.18	3.83	4.00	–
$n_s$	7.5	7.8–8.5	–	6.9	8.8	8.5	–
$K_{\text{for}}$	0.236	0.25–0.28	0.26	0.41	0.185	0.231	0.163–0.188
$n_f$	3	4.5–4.6	3	3	5.7	4.8	3.94–5.02

Notes on modeling parameters:

\*Range of data for different parameters [6].

\*\*Calculations at 50 cm<sup>-1</sup>.

(a) Same as described in Section 3.

(b) Same as in (a) except cut-off = 25 cm<sup>-1</sup>,  $A = 0$  beyond the cut-off.

(c) Same as in (a). The range of data in different windows is shown (see Table 2).

Finally, with respect to a comparison between measured foreign-continuum and theoretically predicted values, we think that we have achieved reasonable agreement with the present experimental results.

A full comparison of absorption coefficients and temperature exponents determined here with other measurements is diminished by the lack of experimental data in the THz region and by the different formalisms used to define the continuum. Different definitions of the continuum present an obstacle because a direct comparison could distort the conclusions unless proper adjustments on their original values have been made in advance. Indeed, if one selects a 25 cm<sup>-1</sup> as the far-wing cut-off in defining local line contributions, the derived continuum values would be larger than those presented here because the latter are based on the 100 cm<sup>-1</sup> cut-off. For example, in the 66.4 cm<sup>-1</sup> window ( $P_{\text{H}_2\text{O}} = 1.43$  kPa,  $P_{\text{N}_2} = 78.5$  kPa,  $T = 323$  K), the local line contributions derived from these 25 and 100 cm<sup>-1</sup> cut-offs differ from each other by 21.5 dB/km. This is a few times larger than the present experimental error.

On the other hand, as long as all the resonance spectrum parameters are well specified as described in Section 3, the adjustment processes can be carried out. A few of the experimental studies assuming the  $\nu^2$ -continuum dependence are summarized in Table 3. All data are converted to (dB/km)/(kPa Hz)<sup>2</sup> and given at the same temperature of  $T = 300$  K. To give an idea on how the choice of parameters may affect the experimentally absorption coefficients and temperature exponents reported here relative to the basic set (with far-wing cut-off of 100 cm<sup>-1</sup> and the upper frequency cut-off of 185 cm<sup>-1</sup>), we present also the data for an additional set of parameters with far-wing cut-off of 25 cm<sup>-1</sup> and the upper frequency cut-off of 110 cm<sup>-1</sup>. In the calculations for this latter set, we still assume a quadratic dependence of the continuum on frequency.

## Acknowledgments

The authors are most grateful to Drs. A. Weber and J. T. Hodges for helpful discussions. This work was supported in part by the NASA Upper Atmospheric Research Grant, NNH05AB21I. Two of the authors (Q. Ma and R. H. Tipping) acknowledge financial support from NASA under Grants NNG06GB23G and FCCS-547. Q. Ma wishes to acknowledge financial support from the Biological and Environmental Research Program (BER), US Department of Energy, Interagency Agreement no. DE-AI02-93ER61744.

## References

- [1] Paine S, Blundell R, Papa DC, Barrett JW, Radford SJE. A Fourier transform spectrometer for measurement of atmospheric transmission at submillimeter wavelengths. *Publ Astronom Soc Pacific* 2000;112:108–18.
- [2] Pardo JR, Cernicharo J, Serabyn E. Atmospheric transmission at microwaves (ATM): an improved model for millimeter/submillimeter applications. *IEEE Trans Antennas Propagat* 2001;49:1683–94.

- [3] Podobedov VB, Plusquellic DF, Fraser GT. Investigation of water-vapor continuum in the THz region using a multipass cell. *JQSRT* 2005;91:287–95.
- [4] Pardo JR, Serabyn E, Cernicharo J. Submillimeter transmission measurements on Mauna Kea during extremely dry El Nino conditions: implications for broadband opacity contributions. *JQSRT* 2001;68:419–33.
- [5] Rosenkranz PW. Water vapor microwave continuum absorption: a comparison of measurements and models. *Radio Sci* 1998;33:919–28.
- [6] Kuhn T, Bauer A, Godon M, Buhler S, Kunzi K. Water vapor continuum: absorption measurements at 350 GHz and model calculations. *JQSRT* 2002;74:545–62.
- [7] Ma Q, Tipping RH. Water vapor millimeter wave foreign continuum: a Lanczos calculation in the coordinate representation. *J Chem Phys* 2002;117:10581–96.
- [8] Burch DE. Absorption of infrared energy by CO<sub>2</sub> and H<sub>2</sub>O. III. Absorption by H<sub>2</sub>O between 0.5 and 36 cm<sup>-1</sup> (278 μ<sup>-2</sup> cm). *J Opt Soc Am* 1968;58:1383–94.
- [9] Hills RE, Webster AS, Alston DA, Morse PLR, Zammit CC, Martin DH, et al. Absolute measurements of atmospheric emission and absorption in the range 100–1000 GHz. *Infrared Phys* 1978;18:819–25.
- [10] Davis GR. The far infrared continuum absorption of water vapor. *JQSRT* 1993;50:673–94.
- [11] White JU. Long optical paths of large aperture. *J Opt Soc Am* 1942;32:285–8.
- [12] Ahonen T, Alanko S, Horneman V-M, Koivusaari M, Paso R, Tolonen A-M, et al. A long path cell for the Fourier spectrometer Bruker IFS 120 HR: application to weak  $\nu_1 + \nu_2$  and  $3\nu_2$  bands of carbon disulfide. *J Mol Spectrosc* 1997;181:279–86.
- [13] Plusquellic DF, Suenram RD, Mate B, Jensen JO, Samuels AC. The conformational structures and dipole moments of ethyl sulphide in the gas phase. *J Chem Phys* 2001;115:3057–67.
- [14] Van Vleck JH, Weisskopf VF. On the shape of collision-broadened lines. *Rev Mod Phys* 1945;17:227–36.
- [15] Waters JW. Absorption and emission by atmospheric gases. *Methods Exp Phys* 1976;12B:142–76.
- [16] Clough SA, Kneizys FX, Davies RW. Line shape and the water vapor continuum. *J Atmos Res* 1989;23:229–41.
- [17] Pardo JR, Serabyn E, Wiedner MC, Cernicharo J. Measured telluric continuum-like opacity beyond 1 THz. *JQSRT* 2005;96:537–45.
- [18] Ma Q, Tipping RH. A simple parameterization for the water vapor millimeter wave foreign continuum. *JQSRT* 2003;82:517–31.